A Constitutive Model for the Forces of a Magnetic Bearing Including Eddy Currents[1]

D. L. Taylor, Associate Professor
K. V. Hebbale [2], Graduate Research Assistant

Sibley School of Mechanical and Aerospace Engineering
Cornell University, Ithaca, New York

ABSTRACT

A multiple magnet bearing can be developed from N individual electromagnets. This paper presents the constitutive relationships for a single magnet in such a bearing. Analytical expressions are developed for a magnet with poles arranged circumferencially. Maxwell's field equations are used so the model easily includes the effects of induced eddy currents due to the rotation of the journal. Eddy currents must be included in any dynamic model because they are the only speed dependent parameter and may lead to a critical speed for the bearing. The model is applicable to bearings using attraction or repulsion.

INTRODUCTION

Research and development activity on passive, active, and combination magnetic bearing systems spans over 150 years beginning with Earnshaw in 1839. The authors will not attempt to summarize the history for this workshop but will simply note research in magnetic bearings, magnetic dampers, and magnetic levitation for vehicles. High speed magnetic bearings are a commercial reality, being used in grinding and polishing machinery, vacuum pumps, compressors, turbines, generators, and centrifuges.

Passive systems using permanent magnets in repulsion are usually incapable of generating sufficient load carrying capacities. Two electromagnetic levitation methods have met with success: direct, position feedback control techniques; and ac modulated or indirect feedback methods. The latter suffers from high eddy current losses and a small range of stable air gaps. Early experiments with fully active systems (1957) were largely thwarted by the then high cost and large size of control system components. Since active magnetic bearings provide both damping and support, and with the reduction in cost and size of sophisticated electronics, the choice is clear. Subsequent efforts for load bearing situations have concentrated on active magnetic bearings.

However, the dynamics of direct feedback magnetic bearings have not been as thoroughly analyzed as have journal bearings. Most of the available literature deals with empirical ideas and concentrates on reliability of the bearing, reducing the size, weight and complexity of the devices. The authors have completed an extensive investigation of the dynamics of an active magnetic bearing [1,2,3,4] in terms of equilibrium points, transient response, on-set of instability, limit cycle size, and forced response. The only speed dependent effect was the change in forces due to eddy currents. This change leads to a critical speed, a Hopf bifurcation with subcritical unstable limit cycles. The reader is referred to [3,4] for a description of the dynamic analysis and results.

The purpose of this paper is to present the eddy current analysis. Although a good analytical model has not previously been available for eddy currents due to shaft rotation, a number of authors have calculated the eddy current effects in other geometrical configurations using a hypothetical simplified model and finite element methods [5,6]. Studies on linear induction motors are available [7,8] which can be extended to magnetic bearings by several assumptions and manipulations. In the above studies, the current density vector is cross multiplied to calculate the induced forces, which does not take care of the attractive force when the moving material is ferromagnetic. In this paper, the forces are calculated using the Maxwell's stress tensor approach which in one calculation gives all the forces involved. Matsumara [9] has derived the fundamental equations for a horizontal shaft magnetic bearing taking into account the rolling, pitching, and yawing of the rotor. In deriving the equations of motion, he assumes that the journal consists of a laminated core and consequently no eddy currents are generated in the material.

FOUR MAGNET BEARING

Consider a bearing using four magnets as shown in Fig. 1. The shaft has high permeability and high conduc-

[1] This work was supported in part by the Office of Naval Research under Contract No. N0014-80-C-0618.

[2] Presently at General Motors Research Laboratories.

tivity and is not laminated. (Lamination would serve to inhibit eddy currents.) Purely for simplicity, all of the four electromagnets are identical, modelled as a coil of N turns on a laminated core of high permeability. Each magnet applies a flux density B_i and the dead weight is suspended by the difference in forces exerted by top and bottom magnets. All magnets generate a flux density which can be adjusted to vary the equilibrium gap lengths under the magnets. This fully energized configuration was chosen so that the magnets could generate the effect of repulsion by decreasing the attraction. The shaft displacement is measured by two coordinates (ξ, η) as shown in Fig. 1, measured from the center of the clearance space in the horizontal and vertical directions respectively when the journal is spinning under the magnets.

If the shaft is not laminated, motion of the conducting shaft through the supporting magnetic fields will induce eddy currents. These eddy currents create two kinds of force on the rotor: drag forces which lead to additional power dissipation and coupling of motions of the journal in two perpendicular directions; and repulsive forces which tend to counter balance the attractive forces and shift the equilibrium point.

The following geometrical assumptions are made. The journal always remains perfectly aligned within the bearing (no tilting). Under small displacements the surfaces of the journal and the magnet pole faces are assumed to remain parallel. Since the individual poles are located at angles $\pm\theta$ relative to the control of the magnet, it is assumed that when the rotor moves vertically a distance η, the change in gap length for the vertical magnets is $\eta cos\theta$. Similarly, when the rotor moves horizontally by a distance ξ, the change in gap length for the horizontal magnets is $\xi cos\theta$. Any other translational motion of the rotor can be written as a superposition of the motions in ξ and η directions. The effect of unequal gap lengths under a vertical magnet caused by a rotor motion in the horizontal direction or vice versa is neglected because the total gap length under that magnet remains constant.

EQUATIONS OF MOTION

The differential equations of motion describing the response of the rotor system require the vectorially combined magnetic forces from all the magnets $\Sigma\vec{F}_{mag}$ at a station along the rotor axis.

$$\sum \vec{F}_{mag} = f(\xi, \eta, \dot{\xi}, \dot{\eta}, B_1, B_2, B_3, B_4) \tag{1}$$

Most rotordynamics codes linearize this to provide the eight bearing coefficients.

$$\begin{pmatrix} F_\xi \\ F_\eta \end{pmatrix} = \begin{bmatrix} c_{\xi\xi} c_{\xi\eta} \\ c_{\eta\xi} c_{\eta\eta} \end{bmatrix} \begin{pmatrix} \dot{\xi} \\ \dot{\eta} \end{pmatrix} + \begin{bmatrix} k_{\xi\xi} k_{\xi\eta} \\ k_{\eta\xi} k_{\eta\eta} \end{bmatrix} \begin{pmatrix} \xi \\ \eta \end{pmatrix} \tag{2}$$

It is immediately obvious that the dynamic characteristics of the bearing are determined by the control system which produces the changes in magnetic flux density. This system may be simply local, represented by

$$B_i = f(\Delta_i, \dot{\Delta}_i) \tag{3}$$

or coupled

$$B_i = f(\xi, \eta, \dot{\xi}, \dot{\eta}) \tag{4}$$

The design of the control system will not be discussed here. Both pole placement methods [4,10] and linear quadratic regulator theory [1] can be used to design state variable controllers.

Each magnet force will be expressed as resolutes normal and tangential to the magnet center line. These forces will include steady state attraction forces and eddy current forces (both repulsion and drag). Only spin velocity is assumed to generate eddy currents. Motion of the journal center $(\dot{\xi}, \dot{\eta})$ doesn't generate eddy currents. The force resolutes are only functions of flux density, gap, and journal speed.

$$F_{ni} = f(\Delta_i, \Omega, B_i) \tag{5}$$

$$F_{ti} = f(\Delta_i, \Omega, B_i) \tag{6}$$

Each magnet gap can be determined from the journal location

$$\Delta_i = f(\xi, \eta) \tag{7}$$

It can then be shown that unless the control is based on velocities

$$c_{\xi\xi} = c_{\xi\eta} = c_{\eta\xi} = c_{\eta\eta} = 0 \tag{8}$$

and the eddy current drag forces produce bearing cross stiffness terms.

Assuming the controller is determined, the general procedure is to:

(a) Determine the equilibrium location for a given spin speed (This assumes no journal velocity, $\dot{\xi} = \dot{\eta} = 0$);
(b) Linearize magnetic forces about equilibrium locations;
(c) Form system dynamic equations, extract eigenvalues, determine stability;
(d) Perform parameter study to locate system bifurcations;
(e) Apply center manifold theorem to determine large amplitude behavior of any bifurcation points;

The usual parameter study would be to follow the equilibrium location and stability as functions of spin speed. Note that due to nonlinearities, the bearing coefficients must be determined at each different parameter value.

MAGNETIC FORCES INCLUDING EDDY CURRENT EFFECTS

The complete eddy current analysis for 4 magnets as shown in Fig. 1 with unequal gap lengths is analytically intractable. (It is probably amenable to finite element techniques.) The following approximations are required.

First, the problem is assumed two dimensional.

Second, the problem will be unwrapped and considered as periodic on a half-space. However, before net forces are calculated, the surface tractions predicted by Maxwell's stress tensor will be wrapped around a circular shaft. As the shaft starts spinning, the eddy currents tend to repel the applied magnetic field and the skin depth of penetration becomes very small. This motivates a semi infinite assumption in the radial direction. The velocity will be treated as constant with respect to y, although it actually decreases linearly as the center is approached. $V = \Omega(\frac{D}{2} + \Delta - y)$. This assumption is supported by the very small skin depth.

Third, each magnet will be considered separately, and the magnetic field for each magnet will be determined individually. The net force of each magnet is then determined, leading to 4 vector forces which are then summed vectorially. An alternative (more complex) solution is discussed later in the paper. Fig. 2 shows the approximate problem to be solved for each magnet.

Fourth, the square wave applied flux density is expanded as a Fourier series

$$B_m(x) = \sum_i \frac{2B_o}{\pi i}[cos(\frac{2bi}{D}) - cos(\frac{2ai}{D})]sin(\frac{2ix}{D}) \tag{8}$$

or

$$B_m(x) = \sum_i B_i sin(k_i x) \tag{9}$$

The field density and current density distributions within the moving material solve a linear problem, and hence the principle of superposition can be invoked and each harmonic handled separately. Figure 3 shows a single harmonic applied to the semi-infinite medium.

The equation that describes the distribution of the magnetic field in the conducting medium is derived from Maxwell's field equations.

$$-\frac{1}{\mu\sigma}\nabla^2\vec{B} + \frac{\partial\vec{B}}{\partial t} = \nabla \times (\vec{V} \times \vec{B}) \tag{10}$$

where $\vec{B} = B_x\vec{e}_x + B_y\vec{e}_y$ ($\vec{e}_x$ and $\vec{e}_y$ being unit vectors in x and y directions respectively). The y component B_y is determined from the y component of (10) The remaining component B_x can be determined from the relation $\nabla \cdot B = 0$. The magnetic field is driven by the applied magnetic field density, and so solutions with the same traveling wave dependence on (x, t) are assumed. That is, it is assumed that the flux density takes the form

$$\vec{B} = [B_x(y)\vec{e}_x + B_y(y)\vec{e}_y]e^{j(kx-\omega t)} \tag{11}$$

The solution form in the y-direction is $e^{\pm qy}$ where

$$q_i = k_i\sqrt{1+js} = k_i\sqrt{1+j\frac{\mu\sigma V}{k_i}} \tag{12}$$

Eqn (12) can be used to predict the skin depth.

The solution domain is divided into two regions, denoted by subscripts 1 and 2 respectively: Region (1), the air gap where $\sigma = 0 (0 \leq y \leq \Delta)$; and Region (2), the moving conducting medium ($\Delta \leq y \leq \infty$). The solutions within each region have two constants of integration, determined from the following 4 boundary conditions:

(1) the applied flux density at $y = 0$;

(2) the solution cannot grow as $y \rightarrow \infty$ (one constant is zero);

(3) conservation of flux at the interface $y = \Delta$ ($\nabla \cdot B = 0$, using the divergence theorem, this leads to $B_{y1} = B_{y2}$).

(4) at the interface, $\nabla \times H = 0$ (using Stokes theorem, this leads to $H_{x1} = H_{x2}$).

Hence, the flux density distribution throughout both regions can be determined.

In the air gap, the solution is

$$\vec{B}_{1i} = \left((D_1 e^{k_i y} + D_2 e^{-k_i y})\vec{e}_x + (D_1 e^{k_i y} - D_2 e^{-k_i y})\vec{e}_y\right) e^{j(k_i x - wt)} \tag{13}$$

where

$$D_1 = \frac{(1 - \frac{\mu_0}{\mu}\frac{q_i}{k_i})B_i e^{-k_i \Delta}}{2[cosh(k_i\Delta) + \frac{\mu_0}{\mu}\frac{q_i}{k_i} sinh(k_i\Delta)]} \tag{14}$$

$$D_2 = \frac{(1 + \frac{\mu_0}{\mu}\frac{q_i}{k_i})B_i e^{k_i \Delta}}{2[cosh(k_i\Delta) + \frac{\mu_0}{\mu}\frac{q_i}{k_i} sinh(k_i\Delta)]} \tag{15}$$

In the journal, the solution is

$$\vec{B}_{2i} = \left(\frac{q_i}{jk_i}\vec{e}_x + \vec{e}_y\right) D_3 e^{-q_i y} e^{j(k_i x - wt)} \tag{16}$$

where

$$D_3 = \frac{B_i e^{q_i \Delta}}{[cosh(k_i\Delta) + \frac{\mu_0}{\mu}\frac{q_i}{k_i} sinh(k_i\Delta)]} \tag{17}$$

The forces acting on the conducting medium are calculated by Maxwell's stress tensor. For magnetic problems with currents and no charges, the forces acting on a body are given by

$$\vec{F} = \int_\Sigma \frac{1}{\mu}[\vec{B}\vec{B} \cdot \vec{n} - \frac{1}{2}\vec{B}^2\vec{n}]dA \tag{18}$$

where Σ is any closed surface surrounding the body and not containing any other body and B is the value of the field on the closed surface. Choosing a closed surface Σ such that it extends from $-\infty$ to ∞ and includes only the conducting medium, the integration is carried out with $\vec{n} = -\vec{e}_y$.

The complete flux density distribution in the whole region of Fig. 2 due to all the applied sinusoidal waves is determined by superposing the individual fields. Each component of the field (B_x, B_y) is an infinite series in sine or cosine terms. The value of the $\vec{B}$ field at the interface, which is required for calculating the forces, is calculated by substituting $y = \Delta$. It is interesting to note that the integral and the summation are interchangable in order. That is, the force for each component of the Fourier series can be determined and then summed or the fields summed and the force determined. This is perhaps surprising because the problem is nonlinear, but the infinite series for B_x and B_y are made up of sine and cosine terms which are orthogonal to one another and all the cross terms drop out during integration over one period.

The total flux can also be calculated and compared with that predicted by magnetic circuit theory (Appendix A). For the numerical example which follows, the more detailed solution is about 8% lower, showing the effects of magnetic circuit assumptions (uniform field density and no leakage in air gap). For comparison to classical problems, the forces for the problem in Fig. 2 will be determined, although the reader is cautioned to go on Eqn. (23) for a bearing problem. Substituting for $\vec{B}$ and evaluating the integrals, the drag and lift forces per unit area acting on the material turn out to be

$$\vec{F}_{drag} = -\frac{1}{4\mu_0}\frac{\mu_0}{\mu}\sum_i \frac{B_i^2}{(n_{1i}^2 + n_{2i}^2)} \frac{s_i}{Re\sqrt{1 + js_i}} \tag{19}$$

$$\vec{F}_{lift} = -\frac{1}{4\mu_0}\sum_i \frac{B_i^2}{(n_{1i}^2+n_{2i}^2)}[1-(\frac{\mu_0}{\mu})^2\sqrt{1+s_i^2}] \tag{20}$$

where

$$s_i = \frac{\mu\sigma V}{k_i} \tag{21}$$

and n_1 and n_2 are the real and imaginary parts of γ_i.

$$\gamma_i = [cosh(k_i\Delta) + \frac{\mu_0}{\mu}\frac{q_i}{k_i}sinh(k_i\Delta)] \tag{22}$$

As expected, when no currents are induced in the slab (V=0,s=0), there is no drag force and the lift is the magnetic attractive force. There is an optimum value of V at which the maximum force per unit area $\vec{F}_x$ is produced. The lift force decreases as V is increased, at some value of V the lift force becomes zero, and at higher values the lift force acts in the opposite direction (repulsion). At very high values of V there is no drag because all the flux is excluded from the material and the repulsion force reaches an asymptotic value irrespective of the permeability of the material.

For the magnetic bearing, the forces acting on a rotating shaft are calculated by wrapping one period of the B field distribution back onto the circular shaft. Choosing a closed surface $\sum$ on the circumference of the rotor and simplifying the integral in Eq. (18) give the forces acting on the rotor per unit width as

$$F_t = -\frac{1}{\mu_0}\int_{-\frac{\pi D}{2}}^{\frac{\pi D}{2}} \tilde{B}_x\tilde{B}_y cos(\frac{2x}{D})dx - \frac{1}{2\mu_0}\int_{-\frac{\pi D}{2}}^{\frac{\pi D}{2}} (\tilde{B}_y^2-\tilde{B}_x^2)sin(\frac{2x}{D})dx \tag{23}$$

$$F_n = -\frac{1}{\mu_0}\int_{-\frac{\pi D}{2}}^{\frac{\pi D}{2}} \tilde{B}_x\tilde{B}_y sin(\frac{2x}{D})dx - \frac{1}{2\mu_0}\int_{-\frac{\pi D}{2}}^{\frac{\pi D}{2}} (\tilde{B}_y^2-\tilde{B}_x^2)cos(\frac{2x}{D})dx \tag{24}$$

where

$$\tilde{B}_x = B_{x1}(y)\Big|_{y=\Delta} = \sum_i -\frac{1}{\gamma_i}\frac{\mu_0}{\mu}\frac{q_i}{k_i}B_i e^{jk_i x} \tag{25}$$

$$\tilde{B}_y = B_{y1}(y)\Big|_{y=\Delta} = \sum_i \frac{1}{\gamma_i}\frac{q_i}{k_i}B_i e^{jk_i x} \tag{26}$$

The parameters in Table 1 were used in the following numerical examples. Figure 4 shows the flux distribution at zero speed and Figure 5 shows the convection effect and decrease in skin depth as velocity increases. Integrating the total flux within the air gap and within the journal, Figure 6 shows how the flux is compressed out of the journal as eddy currents increase. Fig. 7 shows the variation in lift and drag forces. Observe the change over to repulsion at 50,000 rpm. The drag force peaks at a value of 1100 Nt at $\Omega = 10^8 rpm$.

The effect on the values of the forces of the number of terms used in the Fourier series was investigated. The magnetic forces were calculated at different spinning speeds using 10, 25, 50, 100, and 500 terms in the series. Figure 8 shows the variation of the lift force. There is very little change in the results when the number of terms used in the series is 50 or more. There is approximately 3% change in the lift force when the number of terms is increased from 10 to 25 or from 25 to 50. This large number of harmonics is reasonable if the Fourier approximation to the applied square wave is plotted. The drag force effectively converged within 10 harmonics. The authors typically use 25 harmonics in dynamic analysis.

An alternative approach is developed in [2] to find net magnetic field for all four magnets as a single system (simultaneously). The problem is posed in Fig. 9, which shows all four B fields. This complex boundary condition is expanded in a Fourier series and the previous equations applied. However, this approach requires the assumption that all the gaps are equal. At low spinning speeds there is no difference between the two methods as shown in Fig. 10. Only at very high speeds do the two differ. (For parameters in this paper, 4% at 10^5 rpm). Researchers may wish to pursue this method.

CONCLUSION

A very general analytical expression for bearing forces has been presented. The model is applicable to journals made of permeable or nonpermeable material and to DC fields or AC fields. Both kinds of eddy current repulsion bearings are included. The predicted loss of lift (about 30% at 12500 rpm), agrees approximately with experimental results of Yamamura [11]. The expression for the drag force under a single sinusoidal field density wave is the same as that obtained by Meisenholder [9].

Without considering eddy current effects, there is no speed dependent term in the constitutive model for a magnetic bearing. Eddy currents cause a loss of effective lift which can be viewed as an external load and may cause a change in equilibrium point, and change bearing coefficients. More importantly, eddy current drag causes coupling between (x, y). Any change in the x gap affects the drag force in the y direction. Other work has shown this coupling effects bearing stability.

A final comment applies to bearing coefficients (equivalent stiffness and damping matrices). The situation for a magnetic bearing is different from that of journal bearings. It is not possible to determine the 8 classical coefficients just by differentiating the force expressions with respect to $\xi, \eta, \dot{\xi}, \dot{\eta}$. The design of the control system may introduce state variables within the controller. In that case the dynamics of the electrical components must also be incorporated. Some subspace reduction might be possible, but it is impossible to determine even approximate coefficients without a completely designed control system.

REFERENCES

1. Bartlett, R.A.: *Active Vibration Control of Flexible Rotors using Magnetic Bearings*, M.S. Thesis, Cornell University, January 1984.
2. Hebbale, K.V.: *A Theoretical Model for the Study of Nonlinear Dynamics of Magnetic Bearings*, Ph.D. Dissertation, Cornell University, January, 1985.
3. Hebbale, K. and Taylor, D. L.: "Dynamics of a Ferromagnetic Suspension System", proceedings of the 1986 Joint Automatic Control Conference, June 18-20, 1986, Vol. 1, pp. 216-223.
4. Hebbale, K. and Taylor, D. L.: "Nonlinear Dynamics of Attractive Magnetic Bearings", Proceedings of the 1986 Workshop on Bearing Stability, June 2-4, 1986, Texas A&M.
5. Chari, M.V.K.; Silvester, P.P.: "Finite Elements in Electrical and Magnetic Field Problems", John Wiley and Sons, Inc., New York, 1980.
6. Yoshimoto, T.: "Eddy Current Effect in a Magnetic Bearing Model", *IEEE Transactions on Magnetics*, Vol. MAG-19, n5, September, 1983.
7. Meisenholder, S.G.; Wang, T.C.: "Dynamic Analysis of an Electromagnetic Suspension System for a Suspended Vehicle System", TRW Systems Group, Prepared for Federal Railroad Administration, 1972.
8. Wang, T.C.; et. al.: "Single-Sided Linear Induction Motor", Sixth Annual IEEE-IGA Meeting, October, 1971.
9. Matsumara, F.; et. al.: "Fundamental Equation for Horizontal Shaft Bearing and its Control System Design", *Electrical Engineering in Japan*, Vol 101, n3, pp. 123, May-June 1981.
10. Woodson, H.H.; Melcher, J.R.: "Electromechanical Dynamics Part I, Part II", John Wiley and Sons, Inc., New York, 1968.
11. Yamamura, S.; Ito, T.: "Analysis of Speed Characteristics of Attractive Magnet for Magnetic Levitation of Vehicles", *IEEE Transactions on Magnetics*, Vol. MAG-11, n5, Spetember, 1975.

NOMENCLATURE

a	Distance of magnet pole corner (near) from center line
A	Area of magnet pole face.
b	Distance of magnet pole corner (far) from center
B	Magnetic flux density
B_0	Magnetic flux density under the magnet pole
D	Diameter of journal
$\vec{e}$	Unit vectors
F_{mag}	Magnetic force
H	Magnetic field intensity
j	$\sqrt{-1}$
k	Wave number
L	Inductance of circuit

L_i	Flux path length
n_1, n_2	Real and imaginary parts of γ
N	Number of turns in coil
q	Complex wave number
R	Resistance of coil
s_i	Nondimensional velocity
t	Time
$\vec{V}$	Velocity vector
V	Velocity (magnitude)
W_d	Field energy density
W_f	Field energy stored
ξ	shaft displacement
η	shaft displacement
γ	Complex number $= \cosh k\Delta + \mu_0 q/\mu k \sinh k\Delta$
Δ	Gap length
Γ	Magnetomotive force
θ	Magnet pole angle with respect to magnet axis
λ	Flux linkage
μ, μ_r	Permeability
σ	Electrical conductivity of journal material
Σ	Closed surface, Summation sign
Φ	Magnetic flux
Ω	Spin speed of rotor

APPENDIX A
ESTIMATION OF MAGNETIC LIFT FORCE USING CIRCUIT THEORY

If eddy currents are neglected, magnetic circuit theory can be used to approximate the magnetic lift force of a single magnet. The following assumptions are made in deriving the expressions for the magnetic lift force:

1. Field fringing is neglected.
2. Magnetization curve is linear ($B = \mu H$).
3. Magnetic flux density B and field intensity H are uniform over cross-sections of the core, gap, or journal.

An electromagnetic circuit is considered whose elements are gap, core, and journal. Each element has constant crossection A_i and length L_i. The magnetic flux ϕ is assumed constant throughout the circuit, and Γ is the total magnetomotive force within the circuit elements.

The density relationship $\phi = BA$ and the constitutive law $B = \mu H$ can be used to express field intensity in the ferromagnetic material in terms of the field intensity within the air gap.

By definition $\Gamma = \int H dl$ Integrating around the circuit and equating Γ to the current linked (NI) results in an equation for field intensity within the air gap. The field energy is determined within each element $w = \frac{1}{2}\mu H$ and the total field energy is obtained by a volume integral over all the elements.

By definition, the force is the rate of change of stored field energy with respect to the mechanical displacement.

$$F_{mag} = \frac{\mu_0 N^2 A I^2}{(2x + \frac{L_1}{\mu_{r1}} + \frac{L_2}{\mu_{r2}})^2} \tag{A.1}$$

In addition, the total flux ϕ, the magnetic field density B, the magnetic flux linkage λ, and the inductance L can be expressed in terms of the gap length x and current I as:

$$\phi = \frac{\mu_0 N I A}{(2x + \frac{L_1}{\mu_{r1}} + \frac{L_2}{\mu_{r2}})} \tag{A.2}$$

$$B = \frac{\mu_0 N I}{(2x + \frac{L_1}{\mu_{r1}} + \frac{L_2}{\mu_{r2}})} \tag{A.3}$$

$$\lambda = \frac{\mu_0 N^2 I A}{(2x + \frac{L_1}{\mu_{r1}} + \frac{L_2}{\mu_{r2}})} \tag{A.4}$$

$$L = \frac{\mu_0 N^2 A}{(2x + \frac{L_1}{\mu_{r1}} + \frac{L_2}{\mu_{r2}})} \tag{A.5}$$

TABLE 1
Four Magnet Bearing Parameters

JOURNAL		
	Diameter of journal D	= 0.15 m
	Path length in journal L_2	= 0.05 m
	Relative permeability of journal material μ_{r2}	= 100.0
	Electrical conductivity of journal material σ	= 1.0 E+07 mho/m
MAGNET		
	Pole angle	= 15 degrees
	Path length in core L_1	= 0.28 m
	Relative permeability of core material μ_{r1}	= 10000.0
	Area of pole face A	= 0.00025 m^2
	Width of pole face W	= 0.008333 m
	Number of turns N	= 800.0
	Distance of pole corner a	= 0.0075 m
	Distance of pole corner b	= 0.0375 m
	Resistance of coil R	= 3.0 ohms
	Permeability of free space μ_0	= 4π E - 07 H/m

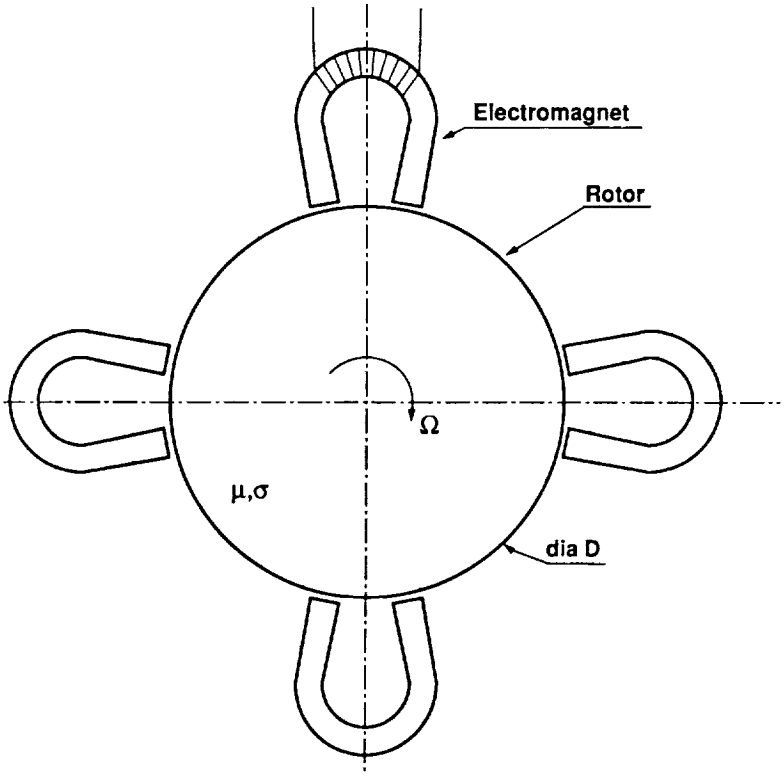

Figure 1. Four magnet bearing.

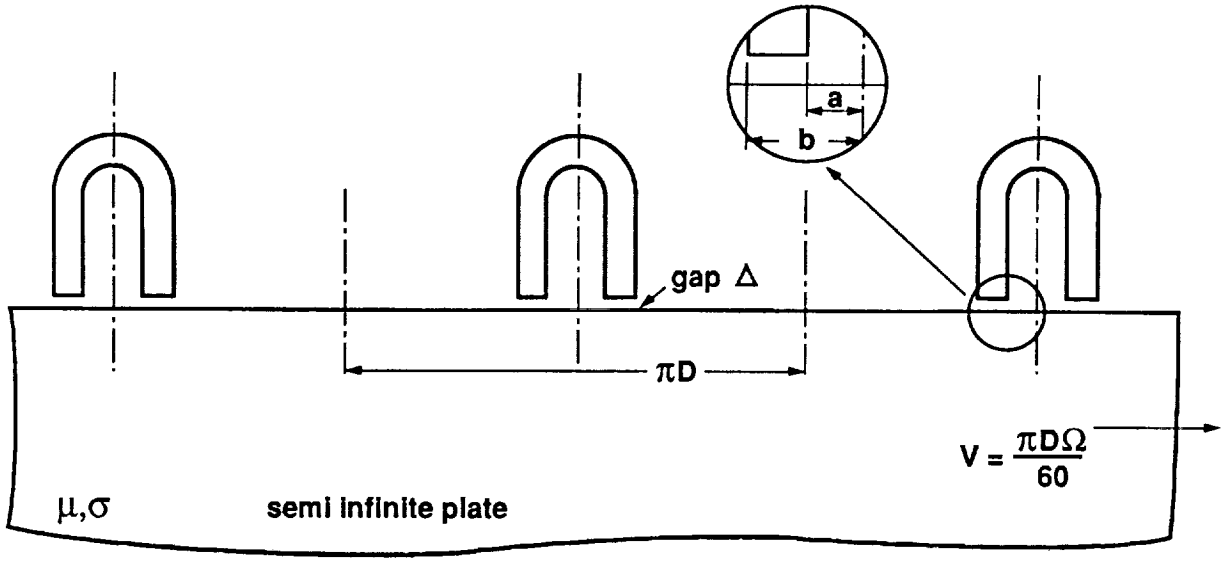

Figure 2. Semi-infinite plane under a series of electromagnets.

C-2

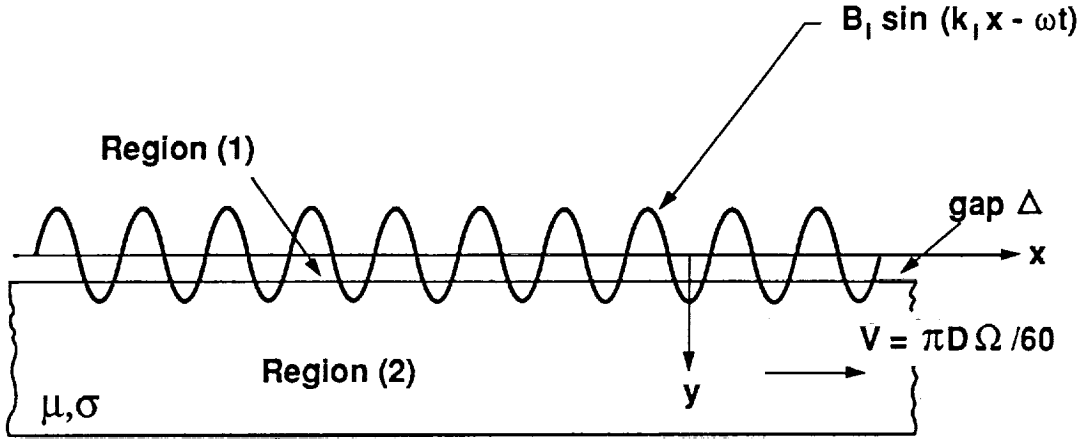

Figure 3. Moving conductive medium under an applied flux density wave.

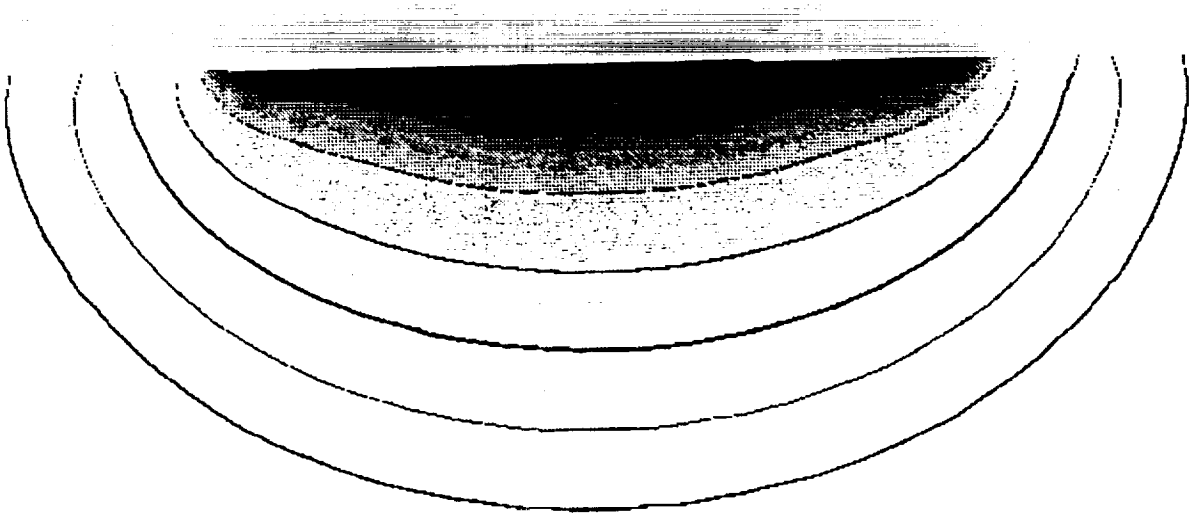

Figure 4. Flux distribution inside stationary conducting medium.

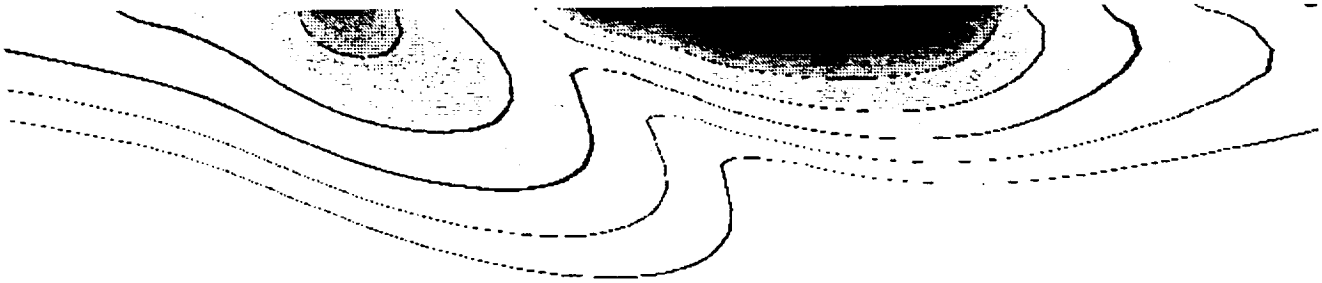

Figure 5. Flux distribution inside moving conducting medium.

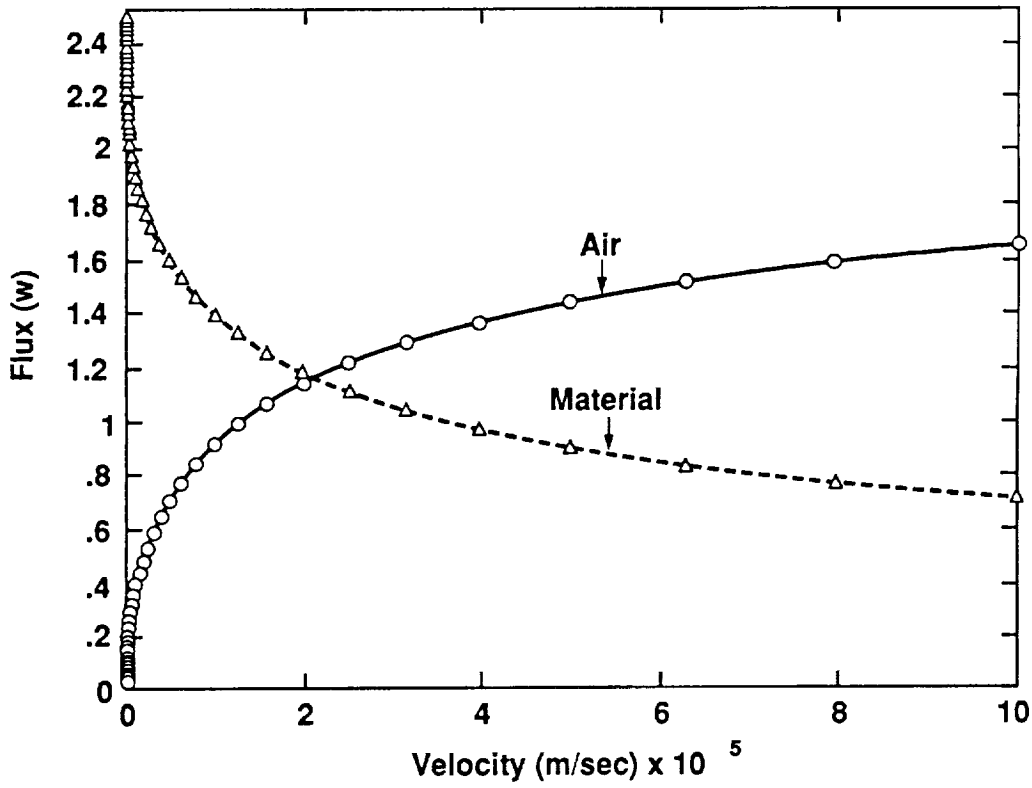

Figure 6. Flux distribution between air gap and journal.

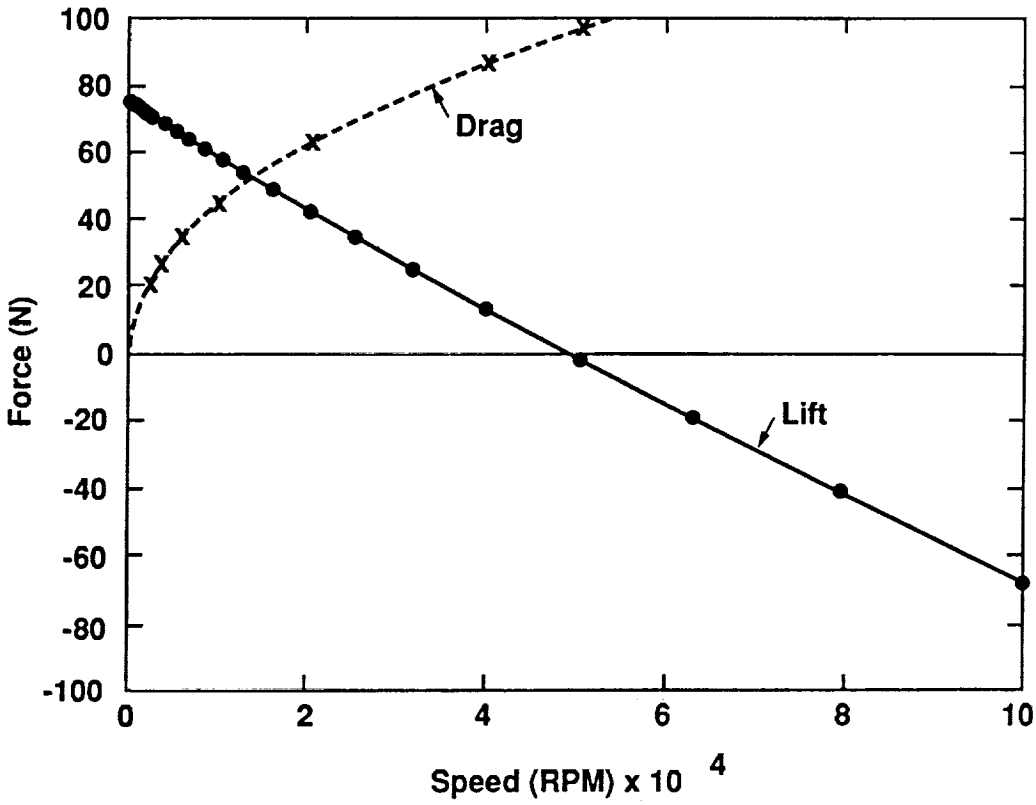

Figure 7. Lift and drag as a function of speed.

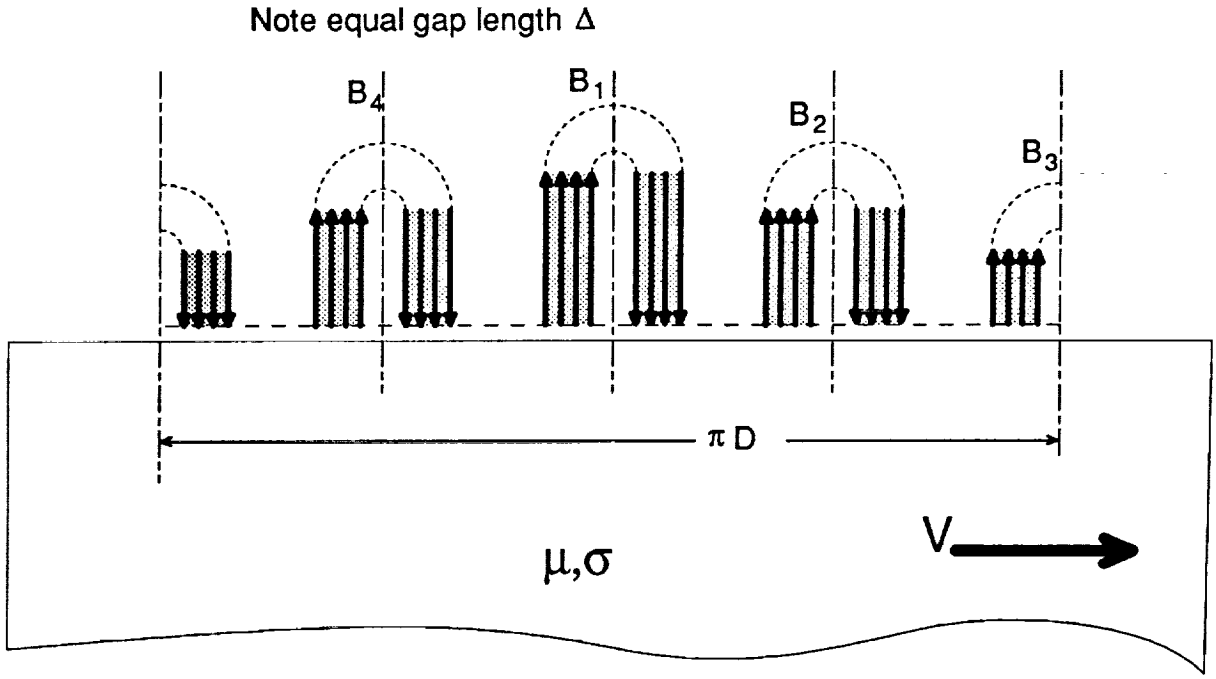

Figure 8. Effect of number of harmonics on lift force.

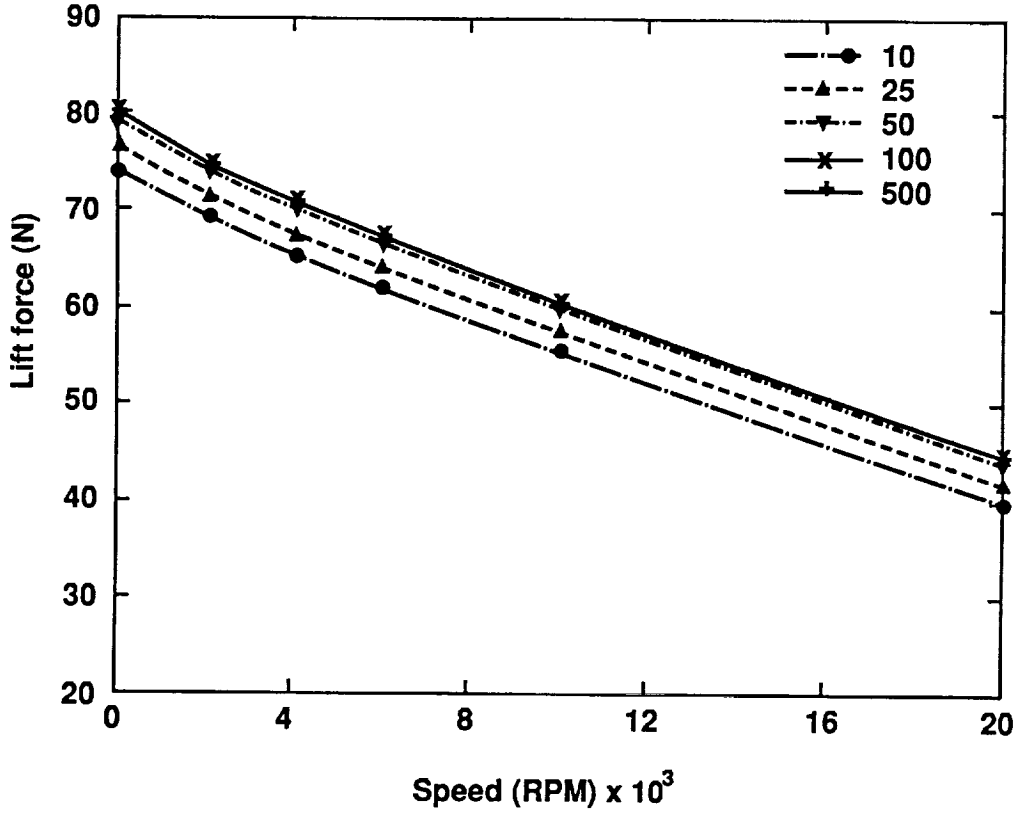

Figure 9. Equivalent problem for multiple magnet case.

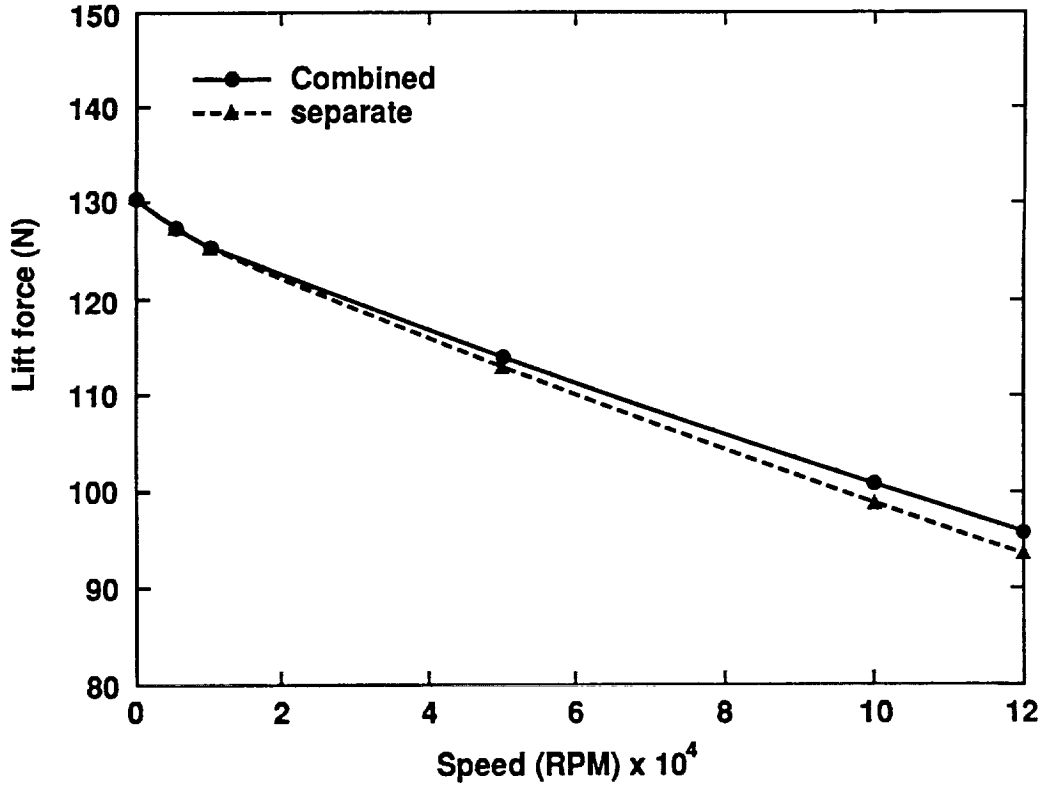

Figure 10. Effect of superposition of lift force.